Effects of contrasting wave conditions on scour and drag on pioneer tidal marsh plants

Reference:

Silinski Alexandra, Heuner Maike, Troch Peter, Puijalon Sara, Bouma Tjeerd J., Schoelynck Jonas, Schröder Uwe, Fuchs Elmar, Meire Patrick, Temmerman Stijn.- Effects of contrasting wave conditions on scour and drag on pioneer tidal marsh plants

Geomorphology - ISSN 0169-555X - 255(2016), p. 49-62

Full text (Publishers DOI): http://dx.doi.org/doi:10.1016/j.geomorph.2015.11.021

Effects of contrasting wave conditions on scour and drag on pioneer tidal marsh plants

Alexandra Silinski[○,a,*], Maike Heuner[○,b], Peter Troch[c], Sara Puijalon[d], Tjeerd J. Bouma[e], Jonas Schoelynck[a], Uwe Schröder[b], Elmar Fuchs[b], Patrick Meire[a], Stijn Temmerman[a]

[a] Ecosystem Management Research Group, University of Antwerp, Universiteitsplein 1C, B-2610 Wilrijk (Antwerp), Belgium.
[b] Federal Institute of Hydrology, Am Mainzer Tor 1, D-56068 Koblenz, Germany.
[c] Dept. of Civil Engineering, Ghent University, Technologiepark Zwijnaarde 904, B-9052 Zwijnaarde (Ghent), Belgium.
[d] UMR 5023 LEHNA, Université Lyon 1, CNRS, ENTPE, Bâtiment Forel, 2ème étage, 43 Boulevard du 11 novembre 1918, F-69622 Villeurbanne Cedex, France.
[e] Royal Netherlands Institute for Sea Research, Korringaweg 7, NL-4401 NT Yerseke, The Netherlands.

[○] first authors

* **Corresponding author at**: Ecosystem Management Research Group, University of Antwerp, Universiteitsplein 1C, B-2610 Wilrijk (Antwerp), Belgium.

Email-address: Alexandra.Silinski@uantwerpen.be (Alexandra Silinski)

Email-addresses of all authors
Heuner@bafg.de;
Peter.Troch@ugent.be;
Sara.Puijalon@univ-lyon1.fr;
Tjeerd.Bouma@nioz.nl;
Jonas.Schoelynck@uantwerpen.be;
Uwe.Schroeder@bafg.de;
Fuchs@bafg.de;
Patrick.Meire@uantwerpen.be;
Stijn.Temmerman@uantwerpen.b

Abstract

Tidal marshes are increasingly valued for protecting shorelines against wave impact, but waves in turn may limit the initial establishment of tidal marsh pioneer plants. In estuaries, the shorelines typically experience a wide range of wave periods, varying from short period wind waves (usually of around 1-2 s in fair weather conditions) to long ship-generated waves, with secondary waves in the order of 2-7 s and primary waves with periods that can exceed 1 minute. Waves are known to create sediment scour around, as well as to exert drag forces on obstacles such as seedlings and adults of establishing pioneer plant species. In intertidal systems, these two mechanisms have been identified as main causes for limiting potential colonization of bare tidal flats. In this paper, we want to assess to which extent common quantitative formulae for predicting local scour and drag forces on rigid cylindrical obstacles are valid for the estimation of scour and drag on slightly flexible plants with contrasting morphology, and hence applicable to predict plant establishment and survival under contrasting wave conditions. This has been tested in a full-scale wave flume experiment on two pioneer species (*Scirpus maritimus* and *Scirpus tabernaemontani*) and two life stages (seedlings and adults of *S. maritimus*) as well as on cylindrical reference sticks, which we have put under a range of wave periods (2-10 s), intended to mimic natural wind waves (short period waves) and ship-induced waves (artificial long period waves), at three water levels (5, 20, 35 cm). Our findings suggest that at very shallow water depths (5 cm) particular hydrodynamic conditions are created that lead to drag and scour that deviate from predictions. For higher water levels (20, 35 cm) scour can be well predicted for all wave conditions by an established formula for wave-induced scour around rigid cylinders. Drag forces can be relatively well predicted after introducing experimentally derived drag coefficients that are specific for the different plant morphologies. Best predictions were found for plants with a simple near-cylindrical morphology such as *S. tabernaemontani*, but are less accurate for plants of more complex structure such as *S. maritimus*, particularly for long period waves. In conclusion, our study offers valuable insights towards predicting/modelling the conditions under which seedlings and shoots of pioneer species can establish, and elucidates that long waves are more likely to counteract successful plant establishment than natural short waves.

Key-words: tidal marshes; colonisation; wave flume experiment; ship waves

1. Introduction

Tidal marshes are valuable ecosystems providing a variety of ecosystem services such as coastal protection by dissipating incoming wave energy and tidal currents (Gedan et al., 2011; Shepard et al., 2011; Temmerman et al., 2013; Möller et al., 2014), carbon sequestration, water purification, maintenance of fisheries, and recreation (Barbier et al., 2011). However, a worldwide decrease of tidal marsh area has been observed over the past decades (e.g. Barbier et al., 2008): tidal marshes are being threatened by conversion into human land-use types from the landward side and by increasing hydrodynamic pressure due to rising sea level and increasing ship traffic from the seaward side, a process known as "coastal squeeze" (Nicholls et al., 1999; Doody, 2004). Previous empirical (Wang and Temmerman, 2013) and modelling studies (Temmerman et al., 2003; Kirwan and Temmerman, 2009; Kirwan et al., 2010; Fagherazzi et al., 2012; Schuerch et al., 2013) on tidal marsh vegetation establishment and survival mainly focused on the effects of vertical marsh elevation relative to mean sea level as a proxy determining tidal marsh vegetation development. However, vertical marsh elevation combines the effects of several variables that more directly determine marsh vegetation growth, such as tidal inundation depth and duration, hydrodynamic forces from tidal currents and waves, and sediment dynamics, which exhibit spatial variation along the horizontal plane.

Several studies highlighted that lateral seaward tidal marsh expansion or landward retreat is at least as important as vertical dynamics in determining tidal marsh evolution (van de Koppel et al., 2005; Fagherazzi et al., 2013). Lateral tidal marsh expansion or retreat are determined by waves and currents as they cause drag forces on plant shoots and cause sediment scour around shoot stems which can eventually lead to uprooting and failure of individual shoots (Bouma et al., 2009, 2005). Hence these hydrodynamic factors affect the lateral expansion of tidal marsh vegetation either by attacking the existing marsh edge as a whole (e.g. Mariotti & Fagherazzi, 2010; Tonelli, Fagherazzi, & Petti, 2010) or by diminishing the chance of seedling or individual shoot establishment and survival on the bare mudflat (Bouma et al., 2009; Callaghan et al., 2010; Balke et al., 2011, 2013). Understanding how tidal marsh vegetation will respond to hydrodynamic impacts such as those caused by waves is thus key to predicting future developments of tidal marshes. In this study we focus on the effect of waves on the establishment of individuals, comparing young seedlings and adults, and comparing species with contrasting mechanical and morphological characteristics that are expected to cause an altered interaction with hydrodynamic forcing and/or turbulence around the stem.

At the scale of an individual plant, waves are episodic high energy events, which, in estuaries, can generally be separated into two groups based on their origin: (i) natural wind-generated waves with regular, short wave periods, typically in the order of 1-2 s in fair weather conditions (Augustin et al., 2009) and (ii) ship-generated waves with a long period primary wave (in the order of 20-120 s) followed by a train of short period secondary waves (in the order of 2-7 s) (Verney et al., 2007; Schroevers et al., 2011). Long period waves can also be generated by wind and storms at sea, but in our study context of a relatively narrow estuary with intensive ship traffic long period waves reaching the shores are mainly generated by ships. While characteristics of wind-generated waves vary over a longer period of time (days, season), ship waves typically arrive on the shores as intense events of several minutes duration (Houser, 2010; Chwang and Chen, 2003). Wind wave characteristics for a given shore morphology depend on wind direction and fetch, while ship wave characteristics depend among others on

relative speed, load and direction of travel of the ship (Chwang and Chen, 2003; Verney et al., 2007; Houser, 2010). This is why in areas with restricted fetch, e.g. in estuaries and lagoons, the wave height, period and energy of ship-generated waves will potentially exceed those of wind waves at the shore (McConchie and Toleman, 2003; Curtiss et al., 2009; Rapaglia et al., 2011), and the tidal marsh vegetation will be exposed to highly contrasting wave conditions.

Waves typically have two effects on pioneer plants, i.e. (i) sediment scouring which determines local erosion around the basal parts of the stems and which can, depending on severity, lead to uprooting (Bouma et al., 2009; Friess et al., 2012) and (ii) drag forces acting on the above-ground plant material (Denny, 1994; Bouma et al., 2005; Henry and Myrhaug, 2013). The combination of scouring and drag forces is considered as the main cause for plant failure, limiting the colonization of the mudflat by plants (Bouma et al., 2009; Balke et al., 2011).

In coastal engineering, wave period has been established as a key parameter to predict wave-generated scour around mono-pile structures: the Keulegan-Carpenter number, KC number in the following, quantifies scour as a function of wave period, flow velocity and the diameter of the structure (e.g. Baglio et al., 2001; Umeda, 2011 and references therein). Drag forces that act on obstacles exposed to a unidirectional flow or waves, on the other hand, have been correlated with the squared flow velocity or squared wave-induced horizontal velocity and wet frontal area of the obstacles, following the Morison equation (Sand-Jensen, 2003; Henry and Myrhaug, 2013, see 2.1). In ecology, the Morison equation has been adapted by introducing a variable power, β, usually referred to as Vogel number (e.g. Sand-Jensen, 2003; Albayrak et al., 2013, see 2.1) which takes the flexibility of plants into account that allows them to reconfigure and thus to reduce experienced drag with increasing flow velocity (Sand-Jensen, 2003; Bal et al., 2011; Puijalon et al., 2011; Pujol and Nepf, 2012; Miler et al., 2014).

While quite a lot of flume experiments on wave impacts on plant performance have been conducted (e.g. Coops et al., 1996; Bouma et al., 2005; Augustin et al., 2009; Francalanci et al., 2013), the novelty of our study is to test the applicability of existing formulae for calculating wave-induced scour and drag forces on plants of differing morphology and for two life stages for a wider range of wave periods and water levels (2-10 s wave periods and 5-35 cm water depths in our experiment versus ranges of maximum 1-2 s and of maximum 20 cm in above-mentioned studies). This has been tested in a full-scale wave flume experiment on two typical pioneer species (*Scirpus maritimus* L. and *Scirpus tabernaemontani* C. C. Gmel.) and two life stages (seedlings and adults of *S. maritimus*). Additionally, wooden cylindrical sticks were tested at the same water levels but at more wave periods (2, 4, 6, 8 and 10 s) acting as uniform control obstacles to which the results for the plants could be compared. The results of these experiments and the identification of valid formulae give us valuable insight for the prediction of potential habitat suitability for the establishment of tidal marsh species under contrasting wave conditions.

2. Material and Methods

2.1 Theory

2.1.1 Hydrodynamic parameters

In order to get an overview on the contrasting hydrodynamic conditions in our experiment, we first introduce hydrodynamic parameters typically used for classification of the governing flow processes.

Reynolds number and Froude number

Reynolds number (Re) determines whether a flow is laminar or turbulent, a value of 2000 being the limit between the two conditions. Froude number (Fr), on the other hand, distinguishes subcritical and hypercritical flow, and 1 is the threshold value. They are defined as (U.S. Army Corps of Engineers, 2002):

$$Re = \frac{v d_{charac}}{\nu} \qquad \text{(eq. 1)}$$

$$Fr = \frac{v}{\sqrt{g d_{charac}}} \qquad \text{(eq. 2)}$$

where v is flow velocity [m.s^{-1}], d_{charac} is characteristic length [m], ν is kinematic viscosity which is equal to 1.004*10^{-6} m^2.s^{-1} for fresh water at 20 °C as used in the experiment, and g is gravitational acceleration, i.e. 9.81 m.s^{-2}.

For *Fr* and *Re*, three different characteristic lengths can be considered in the formula: the hydraulic diameter and flow depth take into account general flow conditions in the flume whereas the use of the cylinder diameter in the formula indicates local flow conditions around the plants and sticks.

Shields parameter

This parameter quantifies the balance between stabilizing and mobilizing forces acting on the sediment (Baglio et al., 2001; Umeda, 2011):

$$\Theta = \frac{\rho v^2}{(\rho_s - \rho) g d_{50}} \qquad \text{(eq. 3)}$$

where v is flow velocity [m.s^{-1}], g = 9.81 m.s^{-2}, ρ is the water density [kg.m^{-3}] = 1000 kg.m^{-3} for fresh water, ρ_s is sediment density [kg.m^{-3}] and d_{50} is the median grain size [m].

Iribarren number

This parameter is commonly used as an indicator for whether or not wave breaking would occur on a plane slope. It is defined as (U.S. Army Corps of Engineers, 2002; Hughes, 2004):

$$\xi_0 = \frac{\tan \alpha}{\sqrt{H_0/L_0}} \qquad \text{(eq. 4)}$$

where α is the slope [°] of our test section ($1/50 \triangleq 1.15$ °), H_0 is the wave height [m] in deep water (i.e. at the wave paddle) and L_0 is the deep water wavelength [m], defined as:

$$L_0 = \frac{g}{2\pi} T^2 \qquad \text{(eq. 5)}$$

with g = 9.81 m.s^{-2} and where T is the wave period [s].

$\xi_0 < 0.5$ defines spilling wave conditions, whereas plunging wave conditions occur for $0.5 < \xi_0 < 3.3$. Surging or collapsing waves require values of $\xi_0 > 3.3$.

2.1.2 Scour

Self-scour around coastal structures such as piles and seawalls is one of the main causes for damage on those structures which is why exhaustive engineering studies have been done in this domain (Sumer et al., 2001). However, scour is a complex matter as it is determined by interactions between properties of the obstacles, hydrodynamics and sediment transport. Scour depends, among others, on Shields parameter, grain size, sediment-to-pile size ratio and pile geometry. In engineering literature, the KC number has established as a reliable predictor for wave-induced scour (Baglio et al., 2001; Sumer et al., 2001; Umeda, 2011 and references therein).

The KC number is calculated as:

$$KC = {}^{Tv}/_{D} \qquad \text{(eq. 6)}$$

where T is the wave period [s], v is the wave-induced horizontal peak forward velocity near the bottom [m.s^{-1}] and D is the diameter of the obstacle [m]. Typically, it is used to predict relative scour, i.e.

$${}^{S}/_{D} \qquad \text{(eq. 7)}$$

where S is maximum scour depth [m] and D is the diameter of the obstacle [m].

2.1.3 Drag forces

The established formula for quantifying the drag force, F [N], exerted by unidirectional flow but also by waves on a rigid object is (e.g. Henry and Myrhaug, 2013):

$$F = \frac{1}{2}\rho C_d A v^2 \qquad \text{(eq. 8)}$$

also known as the Morison equation, where ρ is the density of the fluid [kg.m^{-3}] = 1000 kg.m^{-3} for fresh water as used during our flume experiments, A is the wet frontal area of the obstacle [m^2], C_d is the drag coefficient [-] and v is the flow velocity [m.s^{-1}] in the case of unidirectional flow, or the undisturbed wave-induced horizontal velocity in the case of waves.

For flexible obstacles, typically such as plants, this formula (eq. 8) is modified, according to Vogel (1994), to:

$$F = \frac{1}{2}\rho C_d A v^{\beta} \qquad \text{(eq. 9)}$$

where $0 \leqq \beta \leqq 2$, depending on the flexibility of the plant. β, usually referred to as Vogel number, is typically determined empirically for each plant species individually. The higher the flexibility

of the plant, the smaller β, which implies that drag forces experienced by flexible plants will increase less with increasing flow or wave-induced horizontal velocities as for rigid material such as steel piles. Following Sand-Jensen (2003), β can be determined using eq. 8 by quantifying the experimental drag coefficient that will depend on species as a function of flow velocity, following the formula:

$$C_{d,exp} = av^b \qquad \text{(eq. 10)}$$

where a and b are constants that are empirically derived for each plant species and physical model.

Combined, equations 8 and 10 lead to:

$$F = \frac{1}{2}\rho a A v^{2+b} \qquad \text{(eq. 11)}$$

where a is now the actual drag coefficient and $2+b=\beta$.

$C_{d,exp}$ can also be derived as a function of the local obstacle-induced Reynolds number (Re_D) (Infantes et al., 2011):

$$C_{d,exp} = aRe_D{}^b \qquad \text{(eq. 12)}$$

where a and b, as in eq. 11, are constants that are empirically derived for each plant species and physical model.

2.2 Experimental design

The experiments were conducted in the wave flume facility at the Department of Civil Engineering at Ghent University, Belgium. The flume was 30 m long, 1 m wide and 1.2 m high. The physical model (at real scale, Fig. 1) consisted of a transition slope of 1/20 over 6.8 m, which led to a 12 m-long slope of 1/50. This latter slope is representative for natural tidal marsh-mudflat transition zones in *S. maritimus* and *S. tabernaemontani* dominated pioneer vegetation, for example in the Scheldt Estuary (Belgium and Netherlands) and Elbe Estuary (Germany) (personal observation). A box filled with natural sediment from the Scheldt Estuary (d_{50}=320 µm, non-cohesive) and of 0.3 m depth occupied a stretch of 7 m length of that gently sloping section. A pebble stone absorption beach at the rear end of the flume prevented waves from being reflected. Before each test, the surface of the sediment over the entire test section was brought into the initial slope of 1/50.

The plants and sticks, respectively, were transplanted into this sediment box at a height of 0.5 m above the flume bottom. The plants, either two adults of the same species or two seedlings, were planted at the same locations next to each other, with a distance of approximately 33 cm between them and the respective flume wall. Five replicate runs were done for each tested condition (water depth and wave period at the paddle, see Table 1; each unique water depth-wave period combination will be referred to as "test" in the following), i.e. each on ten plants of the same type. For the stick experiments, only one stick was tested at a time, without replicates.

A regular wave height of 17 cm was set at the paddle for each of the tests but due to wave transformation on the slopes preceding the test section, the actual mean wave heights at the plants and stick varied between 2 and 23 cm, depending on the test (see Table 1). Two regular wave periods were tested on the plants: a 2 s wave period as proxy for natural wind waves, as

can be typically observed in the Scheldt and Elbe Estuary, and a 10 s wave period as an artificially generated long-period wave, representing simplified secondary ship waves. Longer wave periods as for primary ship waves could not be generated due to technical paddle limitations. For the sticks, a series of five wave periods were tested, i.e. 2, 4, 6, 8 and 10 s. Three water levels were chosen (5, 20 and 35 cm relative to the plant and stick position) in order to simulate wave impact at different moments in the tidal cycle or, alternatively, different surface elevation relative to mean high water on the tidal flat. Note that the transformation of waves on the slopes results in asymmetric wave-induced horizontal peak forward and backward velocities, with the backward velocities reaching only 40 to 95 % of the forward velocities: the lower the water level and the shorter the waves, the more asymmetric the velocities with an excess of peak forward velocities. Studies on sediment transport under asymmetric oscillatory flow (e.g. Ruessink et al., 2011; Son and Lee, 2013) predict net forward sediment transport for non-cohesive sand (d_{50} > 200 µm) which was consistent with observations in the flume. Based on field measurements in the Scheldt Estuary, where tidal range is of approximately 5 m, these relatively low inundation depths would prevail on average during around 20 to 40 min in the course of one tidal cycle, depending on the position along the elevation gradient. This is in line with the 7 min (2 s-waves) and 30 min (10 s-waves) test periods that we simulated in the flume experiments. Not all tests were run on all plants: seedlings were only tested at the two lower water levels and the adult *S. tabernaemontani* were only tested at the two higher water levels.

The runs consisted of 200 monochromatic waves for each test. Actual wave heights at the paddle and on the test section were measured for each of the tests with resistance wave gauges (sampling frequency 40 Hz). Mean wave heights (H_{mean}) were calculated (Table 1). Wave-induced horizontal velocities were measured with a laboratory Acoustic Doppler Velocimeter (Nortek Vectrino ADV; Nortek AS, Rud, Norway) at the test section during one run of each test, both close to the sediment bed (8 mm above the sediment bed) and at 1/3 of the respective water column (Table 1). In the analysis, the measured wave-induced horizontal near-bed peak forward velocities were considered for calculations of the scouring (eq. 6) and the wave-induced horizontal peak forward velocities at 1/3 of the water column for the drag forces (eq. 8-12).

2.3 Plant material

60 adult shoots of *Scirpus maritimus* L. as well as 40 adult shoots of *Scirpus tabernaemontani* C. C. Gmel. and 40 seedlings of *S. maritimus* were used in this experiment (Fig. 2). In April 2012, the adult *S. maritimus* and *S. tabernaemontani* shoots were collected from the brackish tidal marshes of the Scheldt Estuary, Belgium (51.36 °N, 4.25 °E, WGS84), and of the Elbe Estuary, Germany (53.84 °N, 9.36 °E, WGS84), respectively. The seedlings were grown from seeds that had been collected in September 2010 at the Belgian location and that had been stored in dry, dark and cool conditions until germination was initiated in early May 2012. The plant material was transplanted into PVC tubes of 0.25 m height and 0.12 m diameter lined with plastic bags and filled with the natural Scheldt sediment that was also used in the flume. Both, adults since April 2012 and seedlings since May 2012, were grown under equal natural outdoor conditions close to the Scheldt Estuary. They were watered with brackish water (5 g $NaCl.L^{-1}$) representative of the natural seasonal field conditions until they were brought to the flume where experiments started end of June 2012.

For transplantation into the flume, the bags containing sediment and roots of the plants could be transplanted and buried into the sand box. Edge effects were avoided by folding the plastic bag downwards and filling up the gap between the sediment of the box and the transplanted root

core. We then measured the plant height and the stem diameter 3 cm above the sediment bed. In a later step, biomechanical properties of plant material from our flume experiment were analysed (Puijalon et al., 2011) in order to better understand the different behaviours of the two plant species and life stages in the different hydrodynamic conditions (see 2.4 and 3.2).

2.4 Measurements of biomechanical traits

We measured biomechanical traits through tensile and bending tests on 19 to 20 replicates for each species and growth form using a universal testing machine (Instron 5942, Canton, MA, USA) (Coops and Van der Velde, 1996; Peralta et al., 2008; Feagin et al., 2011; Möller et al., 2014; Rupprecht et al., 2015). Both tests (tensile and bending) were carried out on each stem: for each test, the stem fragments were 10 cm long for adult plants and 5 cm for seedlings. For each sample, we measured the dimensions of the stem cross-section using a digital calliper (± 0.02 mm) at three different points along the sample: height and width for triangular stem cross-sections (*S. maritimus*) and the shorter and the longer axes for elliptical stem cross-sections (*S. tabernaemontani*).

2.4.1 Bending tests

We performed three-point bending tests, consisting of a force applied at a constant rate of 10 $mm.min^{-1}$ to the midpoint of a sample placed on a support. The following biomechanical traits related to bending were calculated:

- The *Young's modulus* (*E* in Pa) quantifies the material stiffness and is calculated as the slope of the stress-strain curve in the elastic deformation region.
- The *second moment of area* (*I* in m^4) quantifies the distribution of material around the axis of bending, accounting for the effect of the cross-sectional geometry of a structure on its bending stress. *I* was calculated using a formula, depending on the geometry of the cross-section (Niklas, 1992). For triangular cross-sections (*S. maritimus*), $I=(xh^3)/36$, where *x* and *h* are the base and height of the cross-section (m) and for elliptical cross-sections (*S. tabernaemontani*), $I=(\pi/4)yz^3$, where *y* and *z* are the shorter and longer axes of the cross-section.
- The *flexural stiffness* (*EI* in $N.m^2$) quantifies the stiffness of the fragment and was calculated by multiplying *E* and *I*.

2.4.2 Tensile tests

The stem fragments were clamped into the jaws of the testing machine and a constant extension rate of 5 $mm.min^{-1}$ was applied to the upper jaw until they broke. The following biomechanical traits were calculated:

- The *breaking force* (in N) is defined as the maximum force that the sample can bear without suffering mechanical failure.
- The *tensile strength* (in $N.m^{-2}$) is calculated as the breaking force per cross-sectional area.

2.5 Scouring

In order to measure the maximum scouring depth produced around the plant stems at the different wave conditions, we cut off the stems close to the sediment bed after each test, and scanned the sediment surface with a laser scanner (EProfiler developed by Aalborg University, Hydraulic & Coastal Engineering Group, Denmark) with a horizontal grid resolution of 5 mm x 5 mm and with a vertical precision of 1 mm (e.g. De Vos et al., 2012). Reference surfaces next to the plants and sticks, hence outside the influence of self-scour, were also scanned after each test

in order to correct the determined scour depth by any general deformation of the sediment bed without interference with obstacles. These data were imported into a GIS (Esri ArcMap 10.1) where we quantified the scour around each plant and stick in a raster-based analysis with a resolution of 5 mm x 5 mm and where the 95-percentile of maximum scouring depth was considered in order to correct for random extreme values.

2.6 Drag force

Drag forces acting on each of the plants and on the cylindrical sticks under the different hydraulic conditions were measured by means of strain gauges, calibrated for measurements in N, to which we attached the basal part of the cut-off stems and of the cylindrical stick. They were then replanted into the sediment bed at the same location where the plants or sticks had been for the previous run and the respective test was applied once more during approximately 2 minutes. We then extracted 10 peak drag forces from 30 s into the test onwards and averaged them. Wet plant frontal area was determined based on plant morphometric measurements and respective effective water levels (still water level + mean wave amplitude) for the different tests. Based on the Morison equation (eq. 8) we then derived an obstacle-specific drag-coefficient and compared the measured drag forces to the calculated ones (see 2.7 for details.)

2.7 Statistical analysis

Statistical tests were performed with the core-functions of R (R Core Team, 2014) except when stated otherwise. One- and two-way ANOVAs followed by post-hoc Tukey's HSD were performed in order to test significant differences between plant types and water levels. The relation between water level and wave period on wave heights was investigated with Pearson's correlation coefficients. Equally, the correlation of measured relative scour depth and KC numbers, as well as the correlation of wet frontal plant area and experienced drag forces were expressed as Pearson's correlation coefficient.

In order to derive the drag coefficients, $C_{d,exp}$, for the different tested hydrodynamic conditions and different types of obstacles (i.e. plant type or stick), we first derived the correction factor (C_d) required for making the measured and predicted forces (eq. 8) match. As the respective drag coefficient was unknown at this point, we assumed that C_d=1. We then quantified the required drag coefficient for matching measured and predicted forces by deriving the slopes of the linear models forced through the origin (Fig. 6). Note that for the non-forced models, only two (both 5 cm conditions for adults of *S. maritimus*) had an intercept that was significantly different from zero. Moreover, these two intercepts were only marginally different from zero (0.25 and 0.06, respectively). These test- and obstacle-specific drag coefficients were hence our experimentally obtained drag coefficients, $C_{d,exp}$ (Tab. 2). Based on eq. 10 and 12 it was then possible to derive an obstacle-dependent function where $C_{d,exp}$ is expressed per plant type and for the sticks as function of v or Re_D. In order to be able to derive the empirical constants a and b, we fitted non-linear models through the respective points, following the formulae given in eq. 10 and 12, respectively. This was done with the core nls-function in R, for which b is fitted as exponential coefficient and a as linear part. Once a and b were derived, we obtained the actual drag coefficient (a) and could calculate the obstacle-specific variable power, i.e. the Vogel number (β=2+b) (e.g. Sand-Jensen, 2003; Infantes et al., 2011). It needs to be noted that the results obtained for the non-linear fits for the adults based on v have to be seen as hypothetical values, given the small number of points (n=4 for both adult species) on which these model fits are based. For the seedlings, no models could be fitted due to the availability of only 2 data

points after omission of the lowest water level. The goodness of fit was expressed by root mean squared error (RMSE).

Finally, in order to check the validity of the derived drag coefficients in a non-dimensional way, we validated the results from the Morison equation using the respective derived drag coefficients against the actually measured drag forces, where both the calculated and the actually measured drag forces were divided by the respective drag coefficients. In order to validate our corrections, we then performed 10-fold cross-validation and predicted the root mean square prediction error (RMSPE) using the package "cvTools" in R (Alfons, 2012).

3. Results

3.1 Hydrodynamic parameters

We first investigated how water levels and wave periods were related to wave-induced horizontal peak forward velocities and mean wave heights at the test section (Table 1). While wave-induced horizontal peak forward velocities were overall not correlated to water level, they were strongly correlated to wave period for both lower water depth of 5 cm and 20 cm (Pearson's correlation coefficient, r=0.96 and r=0.87, respectively). For the highest water depth of 35 cm, wave period had no significant effect on wave-induced horizontal velocity. Wave height at the test section, on the other hand, increased with water level (Pearson's correlation coefficient, r=0.94), indicating a depth-limited wave condition.

When looking at the hydrodynamic conditions in terms of *Fr*, *Re*, Shields parameter (θ) and Iribarren number (ξ_0) (Table 1), we can state that the long wave period at the shallow water level is the only tested condition for which Fr_d>1, implying a critical combination of shallow water depth and high wave-induced horizontal peak velocity, as well as an outstandingly high Shields parameter (>100), through which this condition might need to be considered as an outlier when analysing our results. Furthermore, the 2 s waves were spilling and 10 s waves plunging at all water levels. .

3.2 Plant properties

Plant height and basal stem diameter did not differ significantly between adults of *S. tabernaemontani* and *S. maritimus* (Fig. 3a). Seedlings, on the other hand, were significantly smaller, with thinner cross-sections than both adult species (Tukey's HSD, p<0.001 for all). Regarding tensile biomechanical properties, both breaking force and tensile strength of seedlings were significantly lower than both adult species (Tukey's HSD, p<0.001 for both, Fig. 3c). For bending properties, seedlings present significantly lower flexural stiffness (i.e. more flexible stems) due to both lower second moment of area and Young's modulus (Tukey's HSD, p<0.05, Fig. 3b). Within the adult species, the stems of *S. tabernaemontani* were less stiff than of *S. maritimus* due to lower Young's modulus (Tukey's HSD, p<0.001, Fig. 3b).

For drag forces, relative inundation at wave passage might have been important. As plant height differed significantly between adults and seedlings (see above), submergence varied with life stage and water level. While both adult species were emergent for all conditions (the plants exceeded two to four times the water level for the high and intermediate water level, respectively, and with adults of *S. maritimus* exceeding the lowest water level by a factor 14), the seedlings were submerged at the intermediate water level, and exceeded the lowest water level only by a factor 3.

3.3 Scour

The KC numbers were significantly correlated to the relative scour produced around the cylindrical sticks at the three water levels and five wave periods (Fig. 4a). There is one outlier, which appears for the test of the long wave period at the shallow water level (i.e. T05.10 in Fig. 4a; after omission of that test, Pearson's correlation coefficient: r=0.90). We accept this condition as an outlier as the applied model does not work for this particular test for which hydrodynamic conditions such as Froude number and Shields parameter were outstandingly high (Fr_d>1, θ>100). The measurements for adults and seedlings of *S. maritimus* at the long wave period of the shallow water level (T05.10 in Fig. 4c) were then equally excluded as outliers, leading to significant correlations (r=0.82 and r=0.86 for adults and seedlings, respectively, after omission of outliers). For *S. tabernaemontani*, correlation is high (r=0.92) for all conditions (Fig. 4b). Apart from the outliers for long waves at shallow water, all plant types followed the same general correlation (overall correlation after omission of the outliers: r=0.86) which implies that the scour depth can be predicted well when wave-induced velocity and wave period are known.

3.4 Drag forces

In terms of the relationship between wet frontal area of the obstacles (sticks or plants) and experienced peak drag forces, figure 5 shows that the stiff sticks followed a clear and simple positive linear correlation according to the theory (Fig. 5a; Pearson's correlation coefficient, r=0.93). The adult plants showed overall also a positive correlation (r=0.81 and r=0.50 for adults of *S. maritimus* and *S. tabernaemontani*, respectively). Seedlings showed an overall weak correlation that was not significant (Fig. 5b, c). At the lowest water level (Fig. 5b), the correlation for the adult *S. maritimus* was also not significant. At the highest water level (Fig. 5d), the observed peak drag forces acting on the plants were clearly lower than expected from the relationship found for the sticks.

However, drag is not only influenced by wet frontal area (eq. 8). A linear model was fitted (see 2.7) between observed and calculated drag forces showing a significant slope ($p<0.001$) for all but three cases and the variance explained (R^2) ranged from 0.46 to 0.85 (Fig. 6 and Table 2). Nevertheless, the calculated drag forces largely underestimated the actually measured drag forces, except for three conditions. That is, in case of seedlings at the shallow and intermediate water level with 10 s waves, and in case of adults of *S. maritimus* at the shallow water level with 10 s waves, the calculated drag forces overestimated the actually observed ones. Based on the linear regression equation between the actually measured and calculated drag forces (Fig. 6), we derived values for $C_{d,exp}$ which are the slope coefficients of the respective linear models (see Table 2).

Comparing the drag coefficients between the different overlapping subsets using ANOVA (e.g. adult *S. maritimus* compared to seedlings of *S. maritimus* at their common water levels, i.e. the two lower water levels), showed that there are no significant differences between both adult species for the common water levels, while both adult species differ significantly from the seedlings ($p<0.001$ when compared to adult *S. maritimus* at the two lower water levels; $p<0.01$ when compared to adult *S. tabernaemontani* at the intermediate water level).

Based on the 10-fold cross-validation performed on the dimensionless validation of the drag force prediction (see 2.7 and Fig. 7), we obtain root mean square prediction errors (RMSPE) of 0.07, 0.21 and 0.25 for adults of *S. tabernaemontani*, adults of *S. maritimus* and seedlings of *S. maritimus*, respectively. The overall RMSPE for all plant types is of 0.19. When only considering

10 s wave periods, adults of *S. tabernaemontani* have an RMSPE of 0.1, adults of *S. maritimus* of 0.24 and seedlings of 0.35. Applying eq. 10 and 11, we derived the actual drag coefficient, a, and the Vogel number, β, from the exponent b (see 2.7 and Table 3, Fig. 8). The results for sticks (Fig. 8a, b) indicate that at the lowest water depth the forces acting on the obstacles were different from the other two water levels, while the two higher water levels showed similar responses. Therefore, we ignored the shallow water depth when fitting the curves for the plants, i.e. the non-linear models for the adults of *S. maritimus* were fit after omission of the shallow water level. Note that the results obtained for a and b have to be understood as hypothetical given the limited amount of points through which the non-linear models were fit for v (n=4 for both adult species).

4. Discussion

Over the last two decades, many flume experiments have been performed on plant-wave interactions (Coops et al., 1996; Bouma et al., 2005; Augustin et al., 2009; Francalanci et al., 2013; Anderson and Smith, 2014) where self-scour and drag forces occurring around and acting on plants – individuals up to marsh scales – have been studied. However, there is a lack of experiments on the contrasting influences of wind and ship waves (i.e. short period and anthropogenically-induced long period waves) on pioneer tidal marsh plants, and of waves in general on drag and scour occurring on plants of differing morphological structures and life stages. The aim of our experiment was to test and validate commonly used formulae for the prediction of scouring and drag forces on typical pioneer marsh plants in the presence of contrasting waves. For further studies, such formulations could then be taken into account when predicting potential habitat suitability for the establishment of intertidal marsh species in an estuary where contrasting hydrodynamic influences, simulated by the wide range of parameters tested in our experiment, occur. However, possible qualitative limitations of our experimental set-up compared to true field conditions (e.g. low water levels and monochromatic waves) need to be considered when drawing conclusions.

While our results show that scour can overall be predicted well for these contrasting conditions with established methods, prediction of drag forces using established methods works well for wind wave conditions (mimicked by 2 s waves) but becomes less accurate for ship-induced waves (mimicked by 10 s waves), especially for plants with a complex morphology such as adults and seedlings of *S. maritimus*. This, in turn, implies that potential habitat suitability in terms of scour under contrasting wave conditions as simulated in the experiment can be predicted in a reliable way, but will be more difficult to assess in terms of drag forces.

Particularity of the shallow water level

The shallow water level produced singular conditions for both scour and drag: the tests on the sticks showed that for all periods of the 5 cm water level, the experimentally obtained drag coefficients were smaller than for the two higher water levels at equal wave-induced horizontal peak forward velocity or Reynolds number (Fig. 8). This indicates that under wave action, there seems to be a threshold of water depth below which the drag forces expected based on wet frontal area and wave-induced horizontal velocities will be smaller than once that water depth threshold is exceeded. In regards to scour, a particularly high Shields parameter was observed for the long wave period at the shallow water level (θ=118.2 vs. an average value of 33.5 ± 5.9 SE after omission of this particular condition), leading to shallower scour depth than expected

based on KC number alone: a high Shields parameter indicates a situation with high mobility of the sediment bed and hence continuous sediment supply; this can then lead to backfilling of local scouring holes, thus reducing the locally observed final scour depth. While this particular observation has also been reported by Umeda (2011), the threshold in water depth for wave-induced drag forces was not reported by other authors. All these particularities found for the sticks were confirmed in the tests with the plants.

Scour

Except for the long wave period at the shallow water level condition, the scour occurring around sticks and plants could be explained largely by the KC number, as suggested by Umeda (2011) for rigid cylindrical obstacles (Fig. 4). However, at equal absolute scour depths, seedlings experienced a deeper relative scour depth (S/D) than adults. As seedlings naturally root less deeply than adult plants, they risk uprooting as the critical scour depth for seedlings will be smaller than for adults. It should also be noted that for both deeper water levels, scour increased with wave period: the ship-generated waves would cause more severe scour than the wind waves, creating thus potentially more critical conditions for plants, especially for seedlings. Overall, the prediction of conditions (i.e. critical combinations of wave periods and flow velocities) that lead to uprooting of plants can be derived based on the KC number.

Drag

Regarding drag forces, the Morison equation (Mendez and Losada, 2004; Bouma et al., 2010; Myrhaug and Holmedal, 2011; Henry and Myrhaug, 2013) leads to fairly good results when each tested condition and plant type is analysed individually (Fig. 6). However, except for the highest water level, the obtained values of the drag coefficients for the 10 s waves were significantly lower than for the 2 s waves, demonstrating that the extreme periods of ship-induced waves lead to a very different behaviour of the plants than under natural wind wave conditions. We found that the application of the experimentally deduced drag coefficients lead to the best results for the adults of *S. tabernaemontani* (Fig. 7d). From this we can draw two main conclusions: (1) it is possible to predict fairly well the expected drag forces to be experienced under wave impact by plants of simple shape such as adults of *S. tabernaemontani* (consisting of oval single stems without leaves), even for extreme wave events; and (2) for plants of more complex structure, such as adults and seedlings of *S. maritimus* (consisting of triangular stems with several leaves), prediction of the expected drag force for wind wave conditions is fairly reliable, while extreme wave events such as potentially ship-induced waves lead to larger inaccuracies of predictions. This is possibly due to the differently acting drag forces on stems on the one hand, and on leaves on the other (Albayrak et al., 2013), where projected leaf surface is overestimating the actually exposed, interfering leaf surface after reconfiguration in the waves. This effect could already be seen based on the results shown in figure 5. Furthermore, the Iribarren number indicates spilling waves for 2 s waves, while the 10 s waves are plunging, pointing at two different wave breaking stages, which could equally have an effect on the dynamics of the wave-induced flow field and hence influence the drag experienced by the more complex plants.

Vogel number and drag coefficient

Following Sand-Jensen (2003), determining the coefficients of equation 10 would lead to the variable power, β, usually referred to as Vogel number and for which typically $0 \leqq \beta \leqq 2$ (e.g.

Bouma et al., 2005; Nepf, 2012; Aberle and Järvelä, 2013). While the overall tendency of the correlations follows the expected relation (i.e. of the type of eq. 10; Fig. 8), the fitted non-linear models for the different plant types (after omission of the shallow water level based on observations for the sticks) lead for both simplest obstacles, i.e. for the sticks and for the adults of *S. tabernaemontani*, to values of β that would be within the expected range. In contrast, we obtain for adults of *S. maritimus* a slightly negative Vogel number (Table 3). This unexpected outcome could first of all result from the limited amount of points to fit the models through (see above), which leads to results that need to be viewed as hypothetical: while the overall tendencies seem valid, the actual numbers might not be correct. Extended experiments for more conditions would help finding more reliable relationships.

As drag coefficients compensate for effects that have not been taken into account by other parameters in the Morison equation, such as the flexibility of the plant type, their value indicates to what point plants or obstacles in general respond in a similar way or not to incoming wave impact. Here it appeared that both adult species, despite their different morphologies and all methodological restrictions, respond – on average – similarly to the incoming waves. The seedlings, on the contrary, given the position of a hypothetical non-linear fit that would lie below the fits of the adults (Fig. 8), respond very differently from the adults, accounting for the differing biomechanical and morphological properties of the life stages, and possibly also due to the stated differences in relative inundation of the plants.

Habitat suitability

According to present results, existing formulas for estimation of expected scour and drag around and on pioneer tidal marsh plants can be applied best for conditions where inundation exceeds a threshold of at least 5 cm, and for natural short wind wave conditions. At more shallow water conditions, both scour and drag will be overestimated by the formulae. This implies that the calculated values for those conditions can be regarded as a worst-case scenario, which is not likely to occur. The morphology of the plants will also affect the reliability of estimated drag, where the simplest plant morphologies will lead to most accurate results. These findings, however, might need to be put into perspective depending on which wave climate prevails in the long term in the field, and which wave climate is apt to create the most extreme forces acting on the plants: in busy shipping estuaries, such as the Scheldt and Elbe Estuaries, a regular interference of long period ship-generated waves can be expected. Furthermore, depending on the prevailing sediment-type in the field, there might be a non-negligible erosion protection provided, at least seasonally, by biofilms and belowground root systems (Le Hir et al., 2007). These could increase the erosion threshold and reduce the resulting scour depth around plants.

When, in a more applied approach, habitat suitability is assessed for pioneer tidal marsh plants in terms of restoration projects, it should nonetheless be considered that, compared to wind waves, a large influence of ship-generated waves will lead to unpredictable drag exerted on plants with complex morphology. At sheltered sites, where wind-generated waves dominate, the conditions will be more reliably predictable.

5. Conclusions

Given the limitations of the presented flume experiment, further investigation (e.g. similar flume studies including stabilisation of the sediment by roots and biofilms) could provide further insights in the actual field processes. Also measuring drag forces and scour produced at higher water levels and possibly under more realistically simulated ship-induced wave events with irregular wave fields would give a better insight in the effects of such waves under normal field conditions. Furthermore, longer test durations, i.e. more than 200 waves, could be considered, and the response of patches of seedlings and shoots, as opposed to effect on individual plants studied here, could be investigated.

Implications from our experiment for life stage and species in terms of environmental suitability for establishment on the intertidal flats are that scour by wind and ship-induced waves will act in a predictable and similar way on all plant types, and KC number is overall a good way for quantifying maximum scouring depth. Ship-induced waves are more likely to create critical conditions, as the scour depth observed after long (i.e., potentially ship-generated) wave periods was significantly deeper than for short (i.e., wind-generated) wave periods. Drag forces experienced under contrasting wave impact, on the other hand, can be well predicted for plants with a simple morphology such as *S. tabernaemontani*, but drag forces acting on plants of more complex structure such as *S. maritimus* will be difficult to predict especially for extreme long period waves. At shallow water levels, the general rules, both for drag and scour, found for higher water levels will fail. Our findings indicate that under contrasting wave periods as typically occurring in many estuaries, habitat suitability for the establishment of pioneer tidal marsh species will be more difficult to assess in the presence of long period, possibly ship-generated waves than in more sheltered, wind wave-dominated conditions.

6. Acknowledgments

This project was financed by the Research Foundation Flanders (FWO, PhD grant to A. Silinski, grant-number 11E0914N), the Port of Antwerp and by the research programme KLIWAS (Impacts of climate change on waterways and navigation - Searching for options of adaptation) of the German Federal Ministry of Transport and Digital Infrastructure (BMVI). The project was further supported by the FWO scientific research community (WOG) on “The functioning of river ecosystems through plant-flow-soil interactions” (grant-number WO.027.11N). We would like to thank B. Koutstaal from NIOZ-Yerseke for growing the plants; T. Versluys and H. Van der Elst from Ghent University for their technical support at the flume; our master thesis student S. Dauwe and three job students for their help and efforts; C. Schwarz for valuable comments on previous versions of this manuscript; E. Fransen from StatUA for advice on the statistics; B. Konz from BfG for artwork; two anonymous reviewers for their constructive and insightful remarks that considerably helped improve the manuscript.

7. References

Aberle, J., Järvelä, J., 2013. Flow resistance of emergent rigid and flexible floodplain vegetation. J. Hydraul. Res. 51, 33–45. doi:10.1080/00221686.2012.754795

Albayrak, I., Nikora, V., Miler, O., O'Hare, M.T., 2013. Flow–plant interactions at leaf, stem and shoot scales: drag, turbulence, and biomechanics. Aquat. Sci. 76, 269–294. doi:10.1007/s00027-013-0335-2

Alfons, A., 2012. cvTools: Cross-validation tools for regression models. R package version 0.3.2.

Anderson, M.E., Smith, J.M., 2014. Wave attenuation by flexible, idealized salt marsh vegetation. Coast. Eng. 83, 82–92. doi:10.1016/j.coastaleng.2013.10.004

Augustin, L.N., Irish, J.L., Lynett, P., 2009. Laboratory and numerical studies of wave damping by emergent and near-emergent wetland vegetation. Coast. Eng. 56, 332–340. doi:10.1016/j.coastaleng.2008.09.004

Baglio, S., Faraci, C., Foti, E., Musumeci, R., 2001. Measurements of the 3-D scour process around a pile in an oscillating flow through a stereo vision approach. Measurement 30, 145–160. doi:10.1016/S0263-2241(00)00064-6

Bal, K.D., Bouma, T.J., Buis, K., Struyf, E., Jonas, S., Backx, H., Meire, P., 2011. Trade-off between drag reduction and light interception of macrophytes: comparing five aquatic plants with contrasting morphology. Funct. Ecol. 25, 1197–1205. doi:10.1111/j.1365-2435.2011.01909.x

Balke, T., Bouma, T., Horstman, E., Webb, E., Erftemeijer, P., Herman, P., 2011. Windows of opportunity: thresholds to mangrove seedling establishment on tidal flats. Mar. Ecol. Prog. Ser. 440, 1–9. doi:10.3354/meps09364

Balke, T., Webb, E.L., van den Elzen, E., Galli, D., Herman, P.M.J., Bouma, T.J., 2013. Seedling establishment in a dynamic sedimentary environment: a conceptual framework using mangroves. J. Appl. Ecol. 50, 740–747. doi:10.1111/1365-2664.12067

Barbier, E.B., Hacker, S.D., Kennedy, C., Koch, E.W., Stier, A.C., Silliman, B.R., 2011. The value of estuarine and coastal ecosystem services. Ecol. Monogr. 81, 169–193. doi:10.1890/10-1510.1

Barbier, E.B., Koch, E.W., Silliman, B.R., Hacker, S.D., Wolanski, E., Primavera, J., Granek, E.F., Polasky, S., Aswani, S., Cramer, L.A., Stoms, D.M., Kennedy, C.J., Bael, D., Kappel, C. V, Perillo, G.M.E., Reed, D.J., 2008. Coastal ecosystem-based management with nonlinear ecological functions and values. Science 319, 321–3. doi:10.1126/science.1150349

Bouma, T.J., De Vries, M.B., Herman, P.M.J., 2010. Comparing ecosystem engineering efficiency of two plant species with contrasting growth strategies. Ecology 91, 2696–704. doi:10.1890/09-0690.1

Bouma, T.J., De Vries, M.B., Low, E., Peralta, G., Tanczos, I., van de Koppel, J., Herman, P.M.J., 2005. Trade-offs related to ecosystem engineering: A case study on stiffness of emerging macrophytes. Ecology 86, 2187–2199. doi:10.1890/04-1588

Bouma, T.J., Friedrichs, M., Klaassen, P., van Wesenbeeck, B.K., Brun, F.G., Temmerman, S., van Katwijk, M.M., Graf, G., Herman, P.M.J., 2009. Effects of shoot stiffness, shoot size and current velocity on scouring sediment from around seedlings and propagules. Mar. Ecol. Ser. 388, 293–297. doi:10.3354/meps08130

Callaghan, D.P., Bouma, T.J., Klaassen, P., van der Wal, D., Stive, M.J.F., Herman, P.M.J., 2010. Hydrodynamic forcing on salt-marsh development: Distinguishing the relative importance of waves and tidal flows. Estuar. Coast. Shelf Sci. 89, 73–88. doi:10.1016/j.ecss.2010.05.013

Chwang, A.T., Chen, Y., 2003. Field measurement of ship waves in Victoria Harbor. J. Eng. Mech. 1138–1148. doi:10.1061/(ASCE)0733-9399(2003)129:10(1138)

Coops, H., Geilen, N., Verheij, H.J., Boeters, R., van der Velde, G., 1996. Interactions between waves, bank erosion and emergent vegetation: an experimental study in a wave tank. Aquat. Bot. 53, 187–198. doi:10.1016/0304-3770(96)01027-3

Coops, H., Van der Velde, G., 1996. Effects of waves on helophyte stands: mechanical characteristics of stems of *Phragmites australis* and *Scirpus lacustris*. Aquat. Bot. 53, 175–185. doi:10.1016/0304-3770(96)01026-1

Curtiss, G.M., Osborne, P.D., Horner-Devine, A.R., 2009. Seasonal patterns of coarse sediment transport on a mixed sand and gravel beach due to vessel wakes, wind waves, and tidal currents. Mar. Geol. 259, 73–85. doi:10.1016/j.margeo.2008.12.009

De Vos, L., De Rouck, J., Troch, P., Frigaard, P., 2012. Empirical design of scour protections around monopile foundations. Part 2: Dynamic approach. Coast. Eng. 60, 286–298. doi:10.1016/j.coastaleng.2011.11.001

Denny, M., 1994. Extreme drag forces and the survival of wind- and water-swept organisms. J. Exp. Biol. 194, 97–115.

Doody, J.P., 2004. "Coastal squeeze" – an historical perspective. J. Coast. Conserv. 10, 129–138. doi:10.1652/1400-0350(2004)010[0129:CSAHP]2.0.CO;2

Fagherazzi, S., Kirwan, M.L., Mudd, S.M., Guntenspergen, G.R., Temmerman, S., Alpaos, A.D., Koppel, J. Van De, Rybczyk, J.M., 2012. Numerical models of salt marsh evolution: Ecological, geomorphic, and climate factors. Rev. Geophys. 50. doi:10.1029/2011RG000359

Fagherazzi, S., Mariotti, G., Wiberg, P.L., McGlathery, K.M., 2013. Marsh collapse does not require sea level rise. Oceanography 26, 70–77. doi:10.5670/oceanog.2013.47

Feagin, R.A., Irish, J.L., Möller, I., Williams, A.M., Colón-Rivera, R.J., Mousavi, M.E., 2011. Short communication: Engineering properties of wetland plants with application to wave attenuation. Coast. Eng. 58, 251–255. doi:10.1016/j.coastaleng.2010.10.003

Francalanci, S., Bendoni, M., Rinaldi, M., Solari, L., 2013. Ecomorphodynamic evolution of salt marshes: Experimental observations of bank retreat processes. Geomorphology 195, 53–65. doi:10.1016/j.geomorph.2013.04.026

Friess, D.A., Krauss, K.W., Horstman, E.M., Balke, T., Bouma, T.J., Galli, D., Webb, E.L., 2012. Are all intertidal wetlands naturally created equal? Bottlenecks, thresholds and knowledge gaps to mangrove and saltmarsh ecosystems. Biol. Rev. Camb. Philos. Soc. 87, 346–66. doi:10.1111/j.1469-185X.2011.00198.x

Gedan, K.B., Kirwan, M.L., Wolanski, E., Barbier, E.B., Silliman, B.R., 2011. The present and future role of coastal wetland vegetation in protecting shorelines: answering recent challenges to the paradigm. Clim. Change 106, 7–29. doi:10.1007/s10584-010-0003-7

Henry, P.-Y., Myrhaug, D., 2013. Wave-induced drag force on vegetation under shoaling random waves. Coast. Eng. 78, 13–20. doi:10.1016/j.coastaleng.2013.03.004

Houser, C., 2010. Relative importance of vessel-generated and wind waves to salt marsh erosion in a restricted fetch environment. J. Coast. Res. 262, 230–240. doi:10.2112/08-1084.1

Hughes, S.A., 2004. Wave momentum flux parameter: a descriptor for nearshore waves. Coast. Eng. 51, 1067–1084. doi:10.1016/j.coastaleng.2004.07.025

Infantes, E., Orfila, A., Bouma, T.J., Simarro, G., Terrados, J., 2011. *Posidonia oceanica* and *Cymodocea nodosa* seedling tolerance to wave exposure. Limnol. Oceanogr. 56, 2223–2232. doi:10.4319/lo.2011.56.6.2223

Kirwan, M., Temmerman, S., 2009. Coastal marsh response to historical and future sea-level acceleration. Quat. Sci. Rev. 28, 1801–1808. doi:10.1016/j.quascirev.2009.02.022

Kirwan, M.L., Guntenspergen, G.R., D'Alpaos, A., Morris, J.T., Mudd, S.M., Temmerman, S., 2010. Limits on the adaptability of coastal marshes to rising sea level. Geophys. Res. Lett. 37. doi:10.1029/2010GL045489

Le Hir, P., Monbet, Y., Orvain, F., 2007. Sediment erodability in sediment transport modelling: Can we account for biota effects? Cont. Shelf Res. 27, 1116–1142. doi:10.1016/j.csr.2005.11.016

Mariotti, G., Fagherazzi, S., 2010. A numerical model for the coupled long-term evolution of salt marshes and tidal flats. J. Geophys. Res. 115, 1–15. doi:10.1029/2009JF001326

McConchie, J.A., Toleman, I.E.J., 2003. Boat wakes as a cause of riverbank erosion: a case study from the Waikato River, New Zealand. J. Hydrol. 42, 163–179.

Mendez, F.J., Losada, I.J., 2004. An empirical model to estimate the propagation of random breaking and nonbreaking waves over vegetation fields. Coast. Eng. 51, 103–118. doi:10.1016/j.coastaleng.2003.11.003

Miler, O., Albayrak, I., Nikora, V., O'Hare, M., 2014. Biomechanical properties and morphological characteristics of lake and river plants: implications for adaptations to flow conditions. Aquat. Sci. doi:10.1007/s00027-014-0347-6

Möller, I., Kudella, M., Rupprecht, F., Spencer, T., Paul, M., van Wesenbeeck, B.K., Wolters, G., Jensen, K., Bouma, T.J., Miranda-Lange, M., Schimmels, S., 2014. Wave attenuation over coastal salt marshes under storm surge conditions. Nat. Geosci. 7, 727–731. doi:10.1038/ngeo2251

Myrhaug, D., Holmedal, L.E., 2011. Drag force on a vegetation field due to long-crested and short-crested nonlinear random waves. Coast. Eng. 58, 562–566. doi:10.1016/j.coastaleng.2011.01.014

Nepf, H.M., 2012. Flow and transport in regions with aquatic vegetation. Annu. Rev. Fluid Mech. 44, 123–142. doi:10.1146/annurev-fluid-120710-101048

Nicholls, R.J., Hoozemans, F.M.J., Marchand, M., 1999. Increasing flood risk and wetland losses due to global sea-level rise: regional and global analyses. Glob. Environ. Chang. 9, S69–S87. doi:10.1016/S0959-3780(99)00019-9

Niklas, K.J., 1992. Plant biomechanics: an engineering approach to plant form and function. University of Chicago Press, Chicago, IL, USA.

Peralta, G., van Duren, L.A., Morris, E.P., Bouma, T.J., 2008. Consequences of shoot density and stiffness for ecosystem engineering by benthic macrophytes in flow dominated areas: a hydrodynamic flume study. Mar. Ecol. Prog. Ser. 368, 103–115. doi:10.3354/meps07574

Puijalon, S., Bouma, T.J., Douady, C.J., van Groenendael, J., Anten, N.P.R., Martel, E., Bornette, G., 2011. Plant resistance to mechanical stress: evidence of an avoidance-tolerance trade-off. New Phytol. 191, 1141–1149. doi:10.1111/j.1469-8137.2011.03763.x

Pujol, D., Nepf, H., 2012. Breaker-generated turbulence in and above a seagrass meadow. Cont. Shelf Res. 49, 1–9. doi:10.1016/j.csr.2012.09.004

R Core Team, 2014. R: A language and environment for statistical computing. Vienna, Austria.

Rapaglia, J., Zaggia, L., Ricklefs, K., Gelinas, M., Bokuniewicz, H., 2011. Characteristics of ships' depression waves and associated sediment resuspension in Venice Lagoon, Italy. J. Mar. Syst. 85, 45–56. doi:10.1016/j.jmarsys.2010.11.005

Ruessink, B.G., Michallet, H., Abreu, T., Sancho, F., Van Der A, D.A., Van Der Werf, J.J., Silva, P.A.,

2011. Observations of velocities, sand concentrations, and fluxes under velocity-asymmetric oscillatory flows. J. Geophys. Res. Ocean. 116, 1–13. doi:10.1029/2010JC006443

Rupprecht, F., Möller, I., Evans, B., Spencer, T., Jensen, K., 2015. Biophysical properties of salt marsh canopies — Quantifying plant stem flexibility and above ground biomass. Coast. Eng. 100, 48–57. doi:10.1016/j.coastaleng.2015.03.009

Sand-Jensen, K., 2003. Drag and reconfiguration of freshwater macrophytes. Freshw. Biol. 48, 271–283. doi:10.1046/j.1365-2427.2003.00998.x

Schroevers, M., Huisman, B.J.A., Wal, M. Van Der, Nortek, B. V, 2011. Measuring ship induced waves and currents on a tidal flat in the Western Scheldt Estuary.

Schuerch, M., Vafeidis, A., Slawig, T., Temmerman, S., 2013. Modeling the influence of changing storm patterns on the ability of a salt marsh to keep pace with sea level rise. J. Geophys. Res. Earth Surf. 118, 84–96. doi:10.1029/2012JF002471

Shepard, C.C., Crain, C.M., Beck, M.W., 2011. The protective role of coastal marshes: a systematic review and meta-analysis. PLoS One 6, e27374. doi:10.1371/journal.pone.0027374

Son, M., Lee, G.H., 2013. On effects of skewed and asymmetric oscillatory flows on cohesive sediment flux: Numerical study. Water Resour. Res. 49, 4409–4423. doi:10.1002/wrcr.20365

Sumer, B.M., Whitehouse, R.J.., Tørum, A., 2001. Scour around coastal structures: a summary of recent research. Coast. Eng. 44, 153–190. doi:10.1016/S0378-3839(01)00024-2

Temmerman, S., Govers, G., Meire, P., Wartel, S., 2003. Modelling long-term tidal marsh growth under changing tidal conditions and suspended sediment concentrations, Scheldt estuary, Belgium. Mar. Geol. 193, 151–169. doi:10.1016/S0025-3227(02)00642-4

Temmerman, S., Meire, P., Bouma, T.J., Herman, P.M.J., Ysebaert, T., De Vriend, H.J., 2013. Ecosystem-based coastal defence in the face of global change. Nature 504, 79–83. doi:10.1038/nature12859

Tonelli, M., Fagherazzi, S., Petti, M., 2010. Modeling wave impact on salt marsh boundaries. J. Geophys. Res. 115, 1–17. doi:10.1029/2009JC006026

U.S. Army Corps of Engineers, 2002. Coastal Engineering Manual. Engineering Manual 1110-2-1110. Washington, D.C. (in 6 volumes).

Umeda, S., 2011. Scour regime and scour depth around a pile in waves. J. Coast. Res. 64, 845–849.

van de Koppel, J., van der Wal, D., Bakker, J.P., Herman, P.M.J., 2005. Self-organization and vegetation collapse in salt marsh ecosystems. Am. Nat. 165, E1–E12. doi:10.1086/426602

Verney, R., Deloffre, J., Brun-Cottan, J.-C., Lafite, R., 2007. The effect of wave-induced turbulence on intertidal mudflats: Impact of boat traffic and wind. Cont. Shelf Res. 27, 594–612. doi:10.1016/j.csr.2006.10.005

Vogel, S., 1994. Life in Moving Fluids; the Physical Biology of Flow, Princeton. ed. Princeton, NJ, USA.

Wang, C., Temmerman, S., 2013. Does biogeomorphic feedback lead to abrupt shifts between alternative landscape states?: An empirical study on intertidal flats and marshes. J. Geophys. Res. Earth Surf. 118, 229–240. doi:10.1029/2012JF002474

Tables

Table 1: Overview of hydrodynamic conditions in the flume. Conditions tested on plants and sticks are indicated in black letters, conditions tested only on sticks are indicated in grey letter. H_{mean} is the average wave height (SE given for replicate tests on plants); v_{peak} bottom is the wave-induced horizontal peak forward velocity measured close to the sediment bed while v_{peak} 1/3 gives the wave-induced horizontal peak forward velocity at 1/3 of the respective water column, and averaged on 20 waves each; subscript h = hydraulic diameter of the flume; d = flow depth; D = diameter of obstacle; Fr_D and Re_D have been calculated based on the diameter of the cylindrical sticks; $\boldsymbol{\theta}$ is the Shields parameter, $\boldsymbol{\xi_0}$ the Iribarren-number; "x" indicates for which tests the respective threshold value, given in the header, is exceeded.

Water depth (cm)	**Wave period (s)**	$\boldsymbol{H_{mean}}$ **± SE (cm)**	$\boldsymbol{V_{peak}}$ **(m/s)**		**Fr_h > 1**	**Fr_d > 1**	**Fr_D > 1**	**Re_h > 2000**	**Re_d > 2000**	**Re_D > 2000**	θ	ξ_0
			bottom	1/3								
5	2	1.9 ± 0.02	0.03	0.11				x			< 0.5	spilling
5	4	2.7	0.07	0.32				x	x		< 5	plunging
5	6	4.4	0.24	0.55				x	x	x	< 50	plunging
5	8	5.6	0.46	0.78			x	x	x	x	< 50	plunging
5	10	3.2 ± 0.48	0.78	0.78		x	x	x	x	x	**> 100**	plunging
20	2	8.8 ± 0.06	0.28	0.15				x	x	x	< 50	spilling
20	4	5.8	0.32	0.24				x	x	x	< 50	spilling
20	6	12.6	0.38	0.36			x	x	x	x	< 50	spilling
20	8	11.7	0.46	0.48			x	x	x	x	< 50	plunging
20	10	14.4 ± 0.42	0.40	0.57			x	x	x	x	< 50	plunging
35	2	18.1 ± 0.19	0.54	0.38			x	x	x	x	< 70	spilling
35	4	12.0	0.57	0.46			x	x	x	x	< 70	spilling
35	6	16.9	0.52	0.42			x	x	x	x	< 70	spilling
35	8	17.9	0.60	0.48			x	x	x	x	< 70	spilling
35	10	23.0 ± 0.86	0.48	0.30			x	x	x	x	< 50	plunging

Table 2: Overview of linear model coefficients (equal to $C_{d,exp}$), obtained for the linear models (with their R^2 and p values) forced through (0,0) between $1/2\rho AC_d v^2$ (with $C_d = 1$) and observed peak drag forces (see Fig. 6); p= 0.05 > * > 0.01 > ** > 0.001 > *** (n=10 for plants, n=1 for sticks).

Water depth (cm)	**Wave period (s)**	**Sticks**	**Adults, *S. mar.***			**Adults, *S. tab.***			**Seedlings, *S. mar.***		
		$C_{d,exp}$	$C_{d,exp}$	R^2	p	$C_{d,exp}$	R^2	p	$C_{d,exp}$	R^2	p
5	2	6.64	8.38	0.58	**	-	-	-	7.02	0.96	***
5	4	9.25	-	-	-	-	-	-	-	-	-
5	6	3.20	-	-	-	-	-	-	-	-	-
5	8	1.57	-	-	-	-	-	-	-	-	-
5	10	0.81	0.56	0.46	*	-	-	-	0.41	0.79	***
20	2	24.79	27.47	0.96	***	22.28	0.97	***	3.23	0.95	***
20	4	11.92	-	-	-	-	-	-	-	-	-
20	6	5.97	-	-	-	-	-	-	-	-	-
20	8	6.53	-	-	-	-	-	-	-	-	-
20	10	3.65	3.07	0.87	***	3.62	0.90	***	0.25	0.60	**
35	2	7.84	4.20	0.86	***	4.59	0.95	***	-	-	-
35	4	6.64	-	-	-	-	-	-	-	-	-
35	6	9.51	-	-	-	-	-	-	-	-	-
35	8	8.12	-	-	-	-	-	-	-	-	-
35	10	12.50	5.55	0.94	***	5.59	0.91	***	-	-	-

Table 3: Summary of determined coefficients (*a, b*) and Vogel number (β) for $C_{d,exp}$ as function of *v* (eq. 10) and Re_D (eq. 12) (see fig. 8), where significance is given by p= 0.1> . > 0.05 > * > 0.01 > ** > 0.001 > *** and with Residual Standard Error (RSE) as measure of goodness of the non-linear fit. na: no statistical output available due to limited number of observations (n).

		V						***Re_D***				
Obstacle	**Condition**	***A***	***b***	***β* (=2+*b*)**	**n**	**p**	**RSE**	***a***	***b***	**n**	**p**	**RSE**
Stick	T05	0.90	-0.97	1.03	5	*	1.0	9.45×10^3	-0.97	5	*	1.0
	T20	1.57	-1.47	0.53	5	**	1.4	1.99×10^6	-1.47	5	**	1.4
	T35	3.32	-1.06	0.94	5	.	1.4	8.22×10^4	-1.06	5	.	1.4
Adult *S. mar.*	T20 & T35	0.45	-2.20	-0.20	4	*	1.3	1.79×10^6	-1.59	40	**	4.1
Adult *S. tab.*	T20 & T35	0.73	-1.83	0.17	4	*	1.4	1.64×10^4	-1.11	40	*	4.9
Seedl. *S. mar.*	T20	-	-	-	2	na	na	1.01×10^3	-0.91	20	**	0.7

Figures

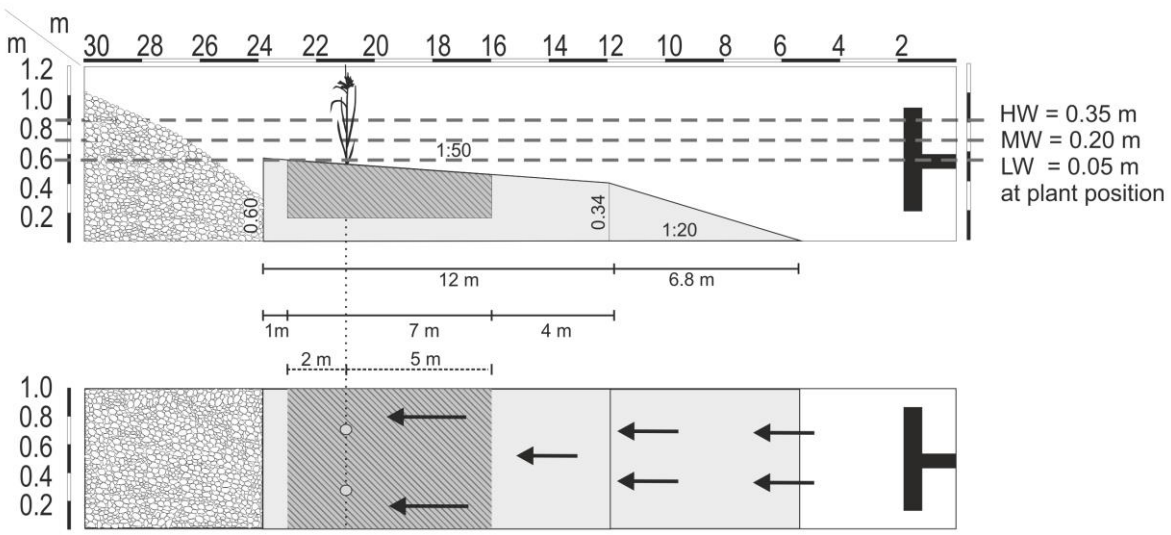

Figure 1: Sketch of the physical model in the wave flume. Top: Side view; bottom: Top view. The position of plants and sticks is indicated by the schematic plant on the top panel and by two light grey circles in the bottom panel. The light grey bodies are the 1/20 transition slope and the 1/50 slope of the test section, which were built of concrete plates. The sediment box (hatched part of the test section) was filled with natural sediments from the Scheldt Estuary (SW Netherlands). The absorption beach (left end of the flume) was built of pebble stones. The horizontal grey dashed lines (top panel) represent the three tested water levels (5, 20 and 35 cm water depth at plant position). The black arrows (bottom panel) represent the direction of propagation of waves produced at the wave paddle (black T-shaped structure on the right end of the flume).

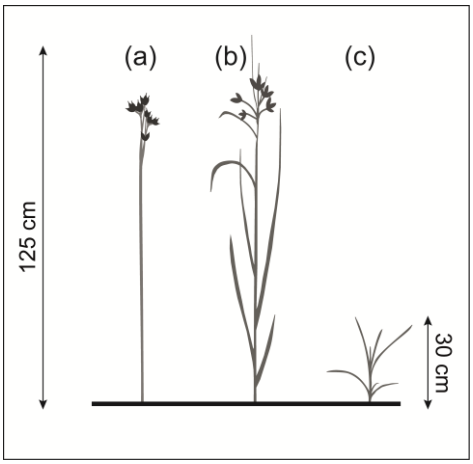

Figure 2: Tested plants. **(a):** adult *S. tabernaemontani*; characteristics: one elliptical stem, no leaves; **(b):** adult *S. maritimus*, characteristics: triangular stem, leaves; **(c):** seedlings of *S. maritimus*, characteristics: small, very flexible, leaves.

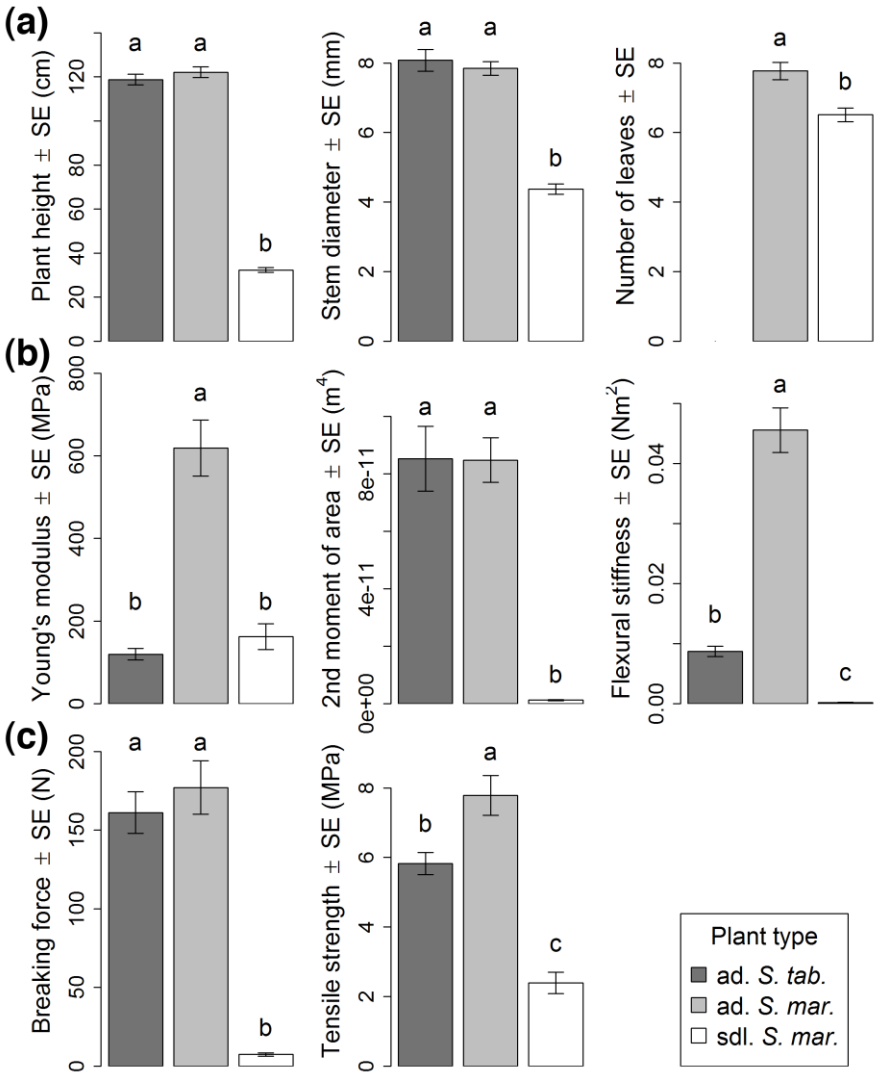

Figure 3: Mean values ± SE of plant properties per plant type: **(a)** Morphological properties as determined on 60 plants for the adult *S. maritimus* and on 40 plants each for adult *S. tabernaemontani* and seedlings of *S. maritimus*; **(b) & (c)** Biomechanical traits of plant stems as determined on 20 stems per plant type: **(b)** Young's modulus, second moment of area and flexural stiffness measured through bending tests; **(c)** breaking force and tensile strength measured through tensile tests. Different letters above the bars indicate significant differences as obtained by a one-way-ANOVA followed by a post-hoc Tukey's HSD.

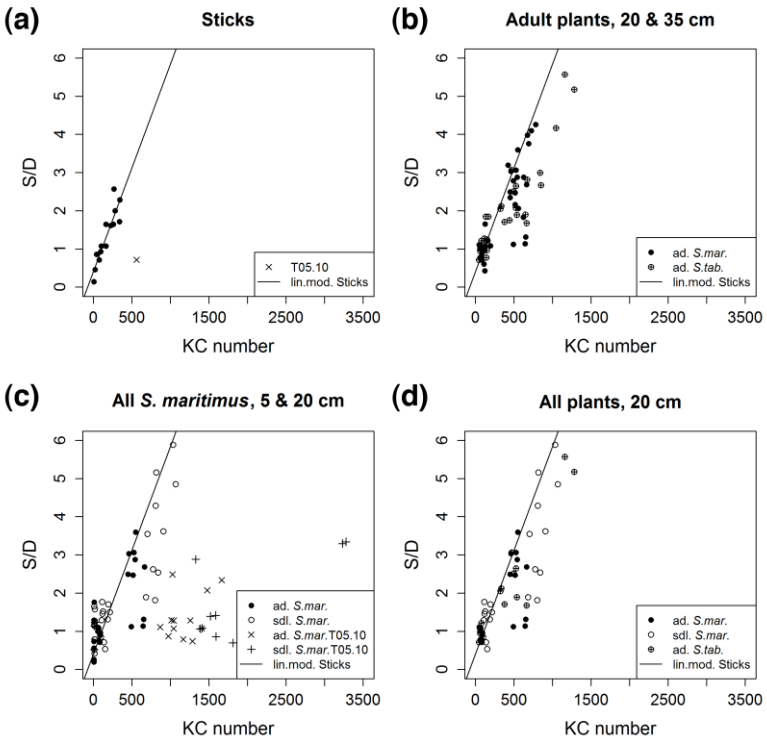

Figure 4: KC number versus relative scour for the sticks **(a)** and the different plant types at equal water levels: **(b)** adult plants at 20 and 35 cm; **(c)** adults and seedlings of *S. maritimus* at 5 and 20 cm; **(d)** all plant types at 20 cm; the linear model shown for the sticks results after omission of the outlier condition for the long wave period at the shallow water level (T05.10).

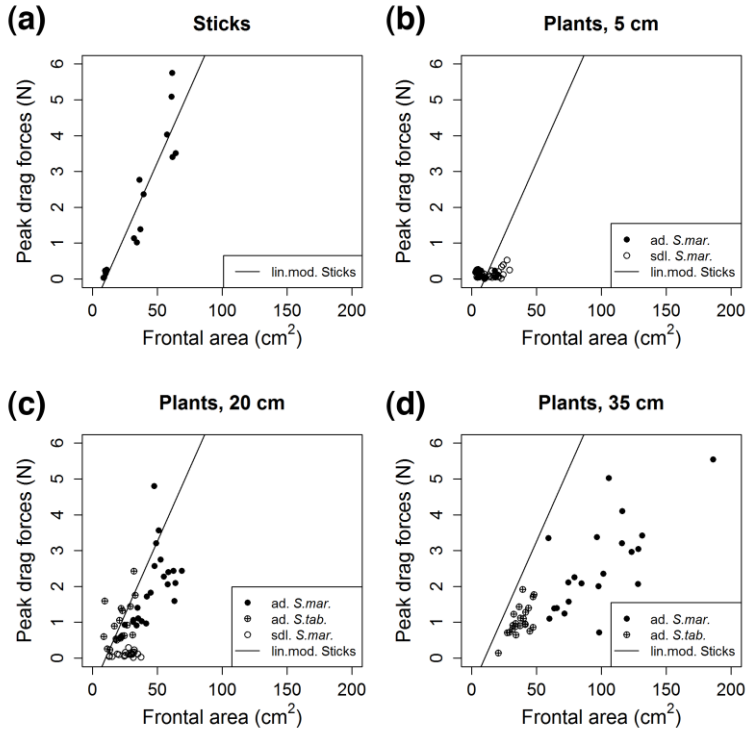

Figure 5: Peak drag forces as function of wet frontal area for the sticks **(a)** and the, respectively, concerned plants at the three tested water levels **(b-d)**. Points represent the observed values and the line represents the regression calculated for the sticks.

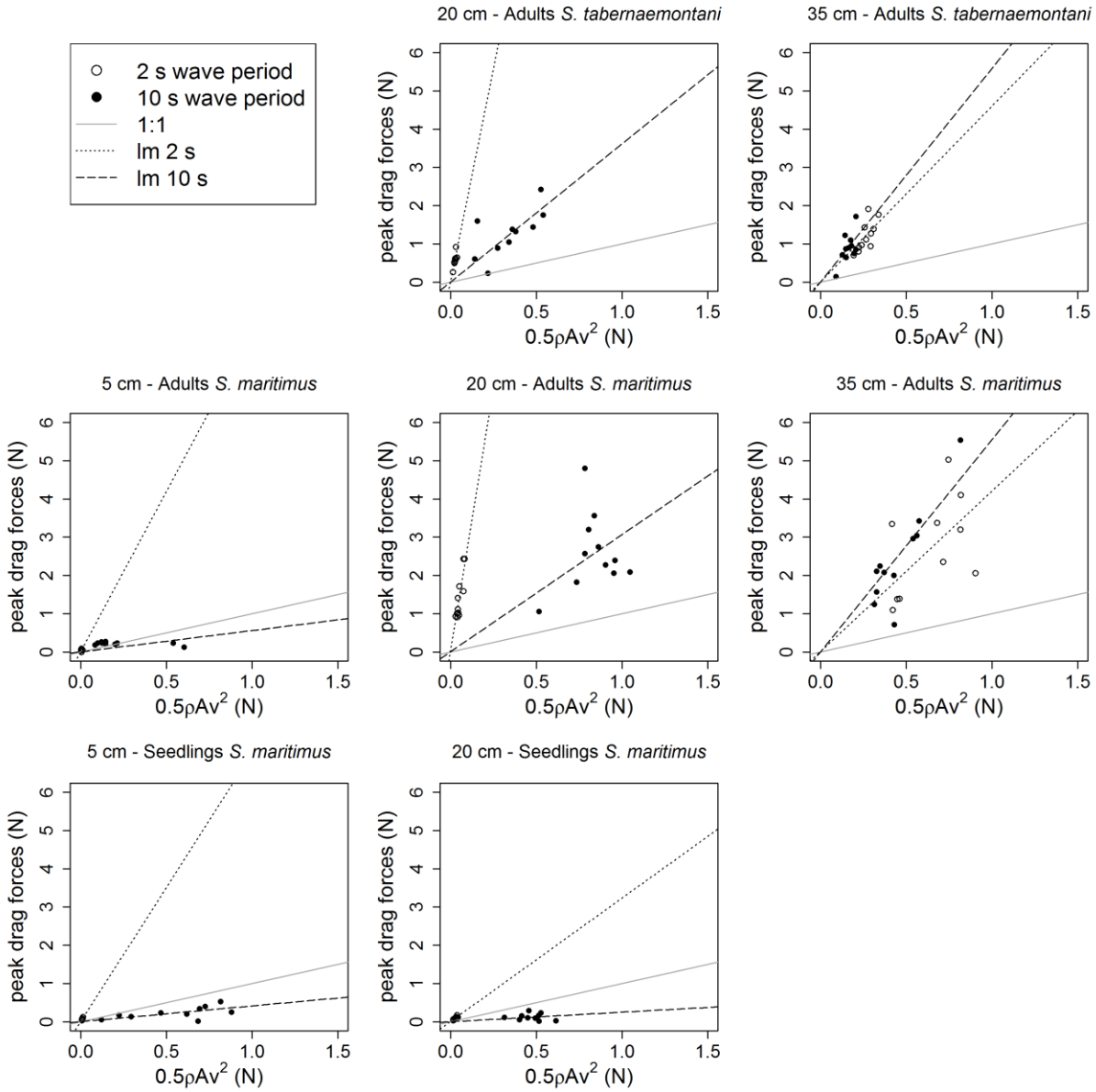

Figure 6: Observed peak drag forces (N) on the three plant types plotted against corresponding drag forces calculated with the Morison equation (eq. 8: $F = 1/2\rho AC_d v^2$ (N)), with C_d=1. From left to right, the three columns show results for the three different water levels; from top to bottom, each of the three plant types is represented in one row; wave periods are distinguished (2 s: hollow circles; 10 s: filled circles); the grey solid line indicates where calculated values correspond to measured values (1:1); the black dotted lines indicate the linear models forced through (0,0) for the 2 s wave conditions, the black dashed lines indicate the linear models forced through (0,0) for the 10 s wave conditions (n=10).

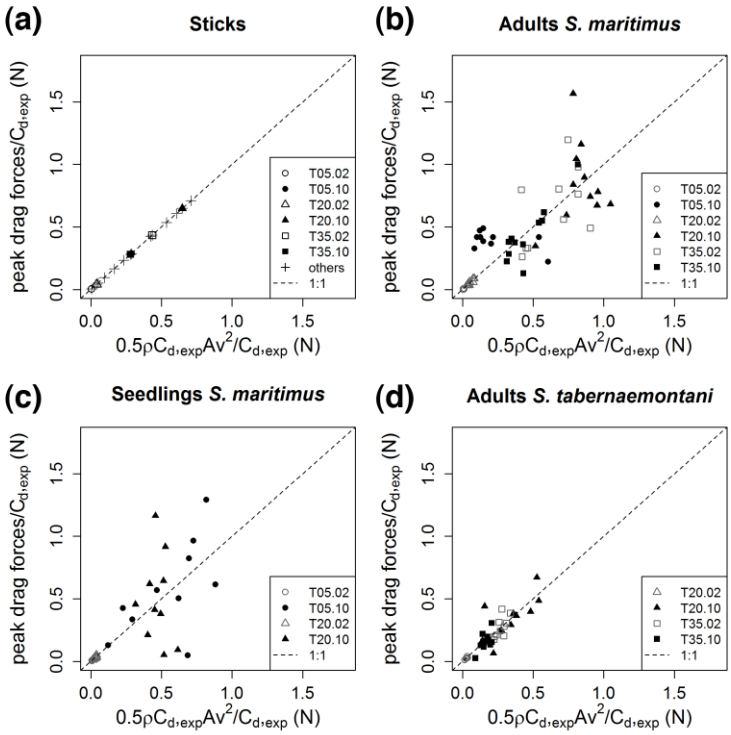

Figure 7: Calculated vs. measured peak drag forces (N) divided by the experimentally obtained drag coefficients for **(a)** the sticks and **(b-d)** the three plant types, respectively.

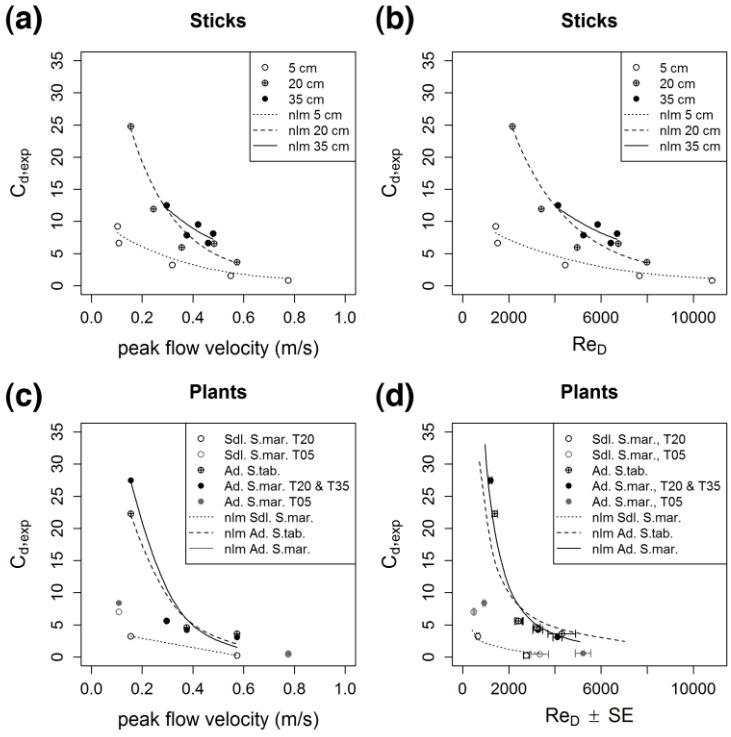

Figure 8: Non-linear fits between the experimentally obtained drag coefficients, wave-induced peak velocities and Re_D; **(a)** and **(b)**: sticks, per water level (n=5); **(c)** and **(d)**: plants, per type where non-linear models for adults of *S. maritimus* were fit after omission of T05 (**for (c):** n=4 for both adults; **for (d):** n=20 for seedlings and n=40 for both adults), which is why the fits in **(c)** need to be considered as hypothetical and the fit cannot be formally tested. The fits in **(d)** remain limited in number of tested conditions performed.